Tunable, high-power, solid-state sources for the blue and ultraviolet

G. K. Samanta[a], A. Esteban-Martin[a], M. Ghotbi[a], M. Ebrahim-Zadeh[*a,b]
[a]ICFO-Institut de Ciencies Fotoniques, Mediterranean Technology Park,
Castelldefels 08860, Barcelona, Spain;
[b]Institucio Catalana de Recerca i Estudis Avancats (ICREA),
Passeig Lluis Companys 23, Barcelona 08010, Spain

ABSTRACT

We describe new sources of tunable, high-power radiation in the blue and ultraviolet. Continuous-wave (cw), single-frequency blue radiation tunable across 425-489 nm and femtosecond ultraviolet (UV) radiation tunable across 250-355 nm is generated by intracavity frequency-doubling of resonant signal radiation in cw and ultrafast optical parametric oscillators (OPOs) in singly-resonant oscillator (SRO) configuration. The cw SRO, pumped in the green, uses a 30-mm MgO:sPPLT as the nonlinear material and a 5-mm BiB_3O_6 (BIBO) crystal for internal doubling. Using this approach, we generate 1.27 W of cw blue power with a linewidth of 8.5 MHz and a TEM_{00} profile. The device also generate a single-frequency signal output of ~100 mW across 850-978 nm and up to 2.6 W of idler power in the 1167-1422 nm spectral range. The femtosecond SRO, based on a 400-μm BIBO crystal and pumped at 415 nm in the blue, can provide visible femtosecond signal pulses across 500-710 nm. Using a 500-μm crystal of β-BaB_2O_4 internal to the SRO cavity, efficient frequency doubling of the signal pulses into the UV is achieved, providing tunable femtosecond pulses across 250-355 nm with up to 225 mW of average power at 76 MHz. Cross-correlation measurements result in UV pulses with durations down to 132 fs for 180 fs blue pump pulses.

Keywords: Optical parametric oscillators, frequency conversion, visible lasers, UV lasers, ultrafast lasers, nonlinear materials

1. INTRODUCTION

Solid-state coherent sources in the blue and UV are of practical interest for applications in optical data storage, laser displays, spectroscopy, medical diagnostics and underwater communication. While cw diode lasers in the blue are available, output power, beam quality, and extended wavelength coverage still remain important limitations. Other well-established techniques, including second harmonic generation (SHG) of near-infrared laser diodes [1] or the short-wavelength transitions in, for example, Nd:YAG [2] and Nd:YVO_4 [3] can provide practical cw powers in the blue, but similarly offer little or no tunability. Frequency doubling of the Ti:sapphire can in principle provide tunable coverage in the 400-500 nm range, but at increased cost and complexity, while similar approaches based on alternative diode-pumped vibronic gain media such as Cr:LiSAF have achieved limited power in the blue over a confined tuning range (427-443 nm) [4]. At the same time, all the described techniques suffer from the common drawback that the attainable spectral range in the blue is ultimately constrained by tunability of the fundamental input lasers, making the 400-500 nm range the current practical limit. On the other hand, the most direct route to generate femtosecond radiation in the UV is external frequency doubling, tripling, or quadrupling of the Kerr-lens mode-locked (KLM) Ti:sapphire laser, which can in principle allow access to spectral regions from below ~200 nm to ~350 nm. While external frequency doubling can provide high output powers at conversion efficiencies in excess 50% over 350-500 nm [5,6], the generation of practical average powers deeper in the UV using single-pass frequency tripling or quadrupling can be limited by low conversion efficiencies [7]. The attainment of tunable coverage in the UV also necessitates wavelength tuning of the KLM Ti:sapphire laser and, furthermore, requires simultaneous adjustment of three tuning parameters, the fundamental wavelength and phase-matching condition in the second and third (or fourth) harmonic processes.

* majid.ebrahim@icfo.es; phone +34 93553 4047 ; fax +34 93553 4000

Nonlinear Frequency Generation and Conversion: Materials, Devices, and Applications VIII, edited by Peter E. Powers,
Proc. of SPIE Vol. 7197, 719702 · © 2009 SPIE · CCC code: 0277-786X/09/$18 · doi: 10.1117/12.808939

Here, we describe an alternative approach to the generation of tunable radiation in the blue and UV in cw and high-repetition-rate femtosecond regimes, which circumvent the limitations of previously established techniques and offer the advantages of wide tuning range, practical output power and efficiency, high spatial, temporal and spectral beam quality, and practical solid-state design. The approach is based on intracavity frequency doubling of cw and synchronously-pumped femtosecond SROs. In the cw regime, we deploy intracavity SHG in a green-pumped, cw, singly-resonant optical parametric oscillator (SRO) based on MgO:sPPLT [8,9], where we generate watt-level, cw, single-frequency blue radiation across 425-489 nm. The approach also offers the important inherent advantage of permitting flexible wavelength coverage beyond the current limits through suitable choice of alternative grating period in the MgO:sPPLT nonlinear gain crystal. In addition to the single-frequency blue output, the SRO generates in excess of ~100 mW of single-mode signal radiation across 850-978 nm and up to 2.6 W of idler in the 1167-1422 nm wavelength range. In the femtosecond regime, we use intracavity frequency doubling in a visible synchronously-pumped SRO based on BiB_3O_6 (BIBO) pumped at 415 nm by a KLM Ti:sapphire laser in the blue [10] for the UV generation. The approach offers major advantages over, for example, external enhancement doubling of the OPO output [11]. These include the use of only one synchronous cavity and no need for active length control or input coupling optimization of the enhancement cavity, resulting in reduced complexity. Our approach also provides a conversion efficiency of 83% from usable OPO output to the UV, compared to 53% in external enhancement doubling [11]. Using this technique, we demonstrate tunable femtosecond pulses across the 250-355 nm in the UV at practical average output powers up to 225 mW. The blue-pumped BIBO OPO is a uniquely versatile source of femtosecond pulses with wide and continuous tunability across the visible using collinear phase-matching. Similar attempts based on BBO using non-collinear pumping had previously resulted in substantially lower output power and limited tuning range of 76 nm in the visible [12]. The use of non-collinear pumping in BBO can result in gain degradation and confined tuning range, as well as beam pointing variation across the OPO tuning range. These, together with the lower nonlinearity of BBO in the visible, render this approach inefficient, offering limited output power and wavelength coverage in the UV.

2. GENERATION OF TUNABLE CW BLUE RADIATION

2.1 Experimental configuration

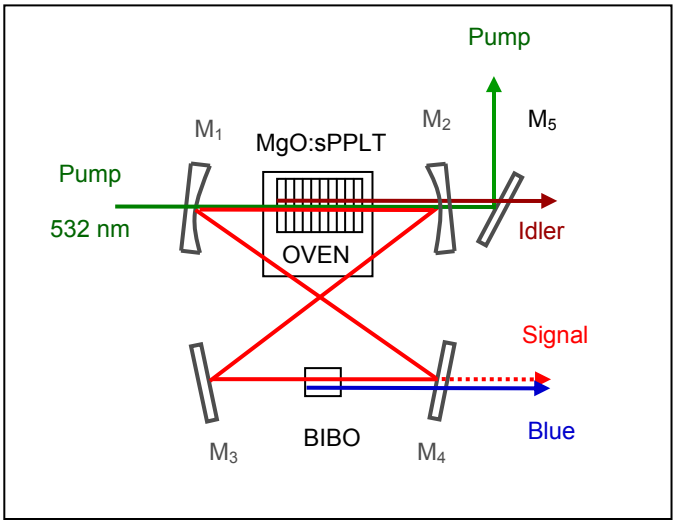

Fig. 1. Schematic of the intracavity frequency-doubled MgO:sPPLT cw SRO for blue generation.

The configuration of the cw SRO (Fig. 1) is similar to that described in Ref. [9]. The cavity is formed in a ring, comprising two concave reflectors, M_1 and M_2 (r=50 mm), and two plane mirrors, M_3 and M_4. Limited by physical constraints, the angle of incidence on M_1 and M_2 is kept <7.5° to minimize astigmatism. The mirrors M_1, M_2 and M_3 are all highly reflecting (R>99.9%) for the resonant signal (840-1000 nm). Mirror M_4 also has high reflectivity for the signal (R>99% over 850-920nm, R>99.9% over 920-1000 nm), and high transmission (T=85-90%) over 425-500 nm. All mirrors are also highly transmitting (T=85-90%) for the idler (1100-1400 nm), thus ensuring SRO operation. The nonlinear crystal is MgO:sPPLT (d_{eff}~10 pm/V). It is 30-mm long, contains a single grating (Λ=7.97 μm), and is housed in an oven with a temperature stability of ± 0.1 °C. The crystal faces have antireflection (AR) coating (R<0.5%) for the signal (840-1000 nm), with high transmission (T>98%) for the pump at 532 nm. The residual reflectivity of the coating is 0.6% to 4% per face for the idler (1100-1400 nm). The pump source is a frequency-doubled, cw, single-frequency Nd:YVO_4 laser, as described previously [8,9].

For internal SHG, we used BiB_3O_6 (BIBO) as the nonlinear crystal due to its high nonlinear efficiency and low spatial walkoff [5,13]. The crystal is 5 mm in length and 4 mm × 8 mm in aperture. It is cut for type I phase matching ($ee \rightarrow o$) in the optical yz-plane (φ=90°) at an internal angle θ=160° at normal incidence (d_{eff}~3.4 pm/V), corresponding to a fundamental wavelength of ~920 nm. The crystal end-faces are AR-coated for the resonant signal (R<0.5% over 850-1000 nm) and the SHG wavelengths (R<0.8% over 425-500 nm). For the SRO, we use a relatively strong pump focusing parameter of ξ_{SRO}=2, corresponding to a pump beam radius of w_{op}=24 μm inside the MgO:sPPLT crystal [8,9]. The signal beam waist is w_{os}~31 μm, resulting in optimum mode-matching to pump (b_s=b_p).The BIBO crystal is located at the second cavity focus between M_3 and M_4. The signal waist at the centre of the crystal is ~160 μm, corresponding to a focusing parameter ξ_{SH}~0.015. Such loose focusing was used to ensure an effective interaction length in BIBO, limited by spatial walkoff, equal to or longer than the crystal length. The total optical length of the cavity including both the crystals is 298 mm, corresponding to FSR ~1.01 GHz. Unlike our previous work [9], the SRO cavity here does not include an intracavity etalon.

2.2 Tuning of intracavity frequency-doubled CW SRO in the blue

Figure 2 shows the SRO tuning range in the signal and idler and the generated blue wavelength as functions of crystal temperature. The wavelengths were measured using a wavemeter (Burleigh, WA-1000) with a resolution of 1 pm. The SRO could be continuously tuned over 978-850 nm in the signal and 1167-1422 nm in the idler by varying the crystal temperature from 71°C to 240°C. Thus, the tuning was continuous over 850–1422 nm, except for a gap near degeneracy (978-1167 nm) due to the reflectivity fall of SRO mirrors to prevent doubly-resonant oscillation. The limit to SRO tuning at the extremes of the signal and idler range was set by the maximum operating temperature of the oven at 240°C. The corresponding SHG wavelengths from 489 to 425 nm are generated by varying the internal angle of the BIBO crystal from 163.8° to 155.2°.

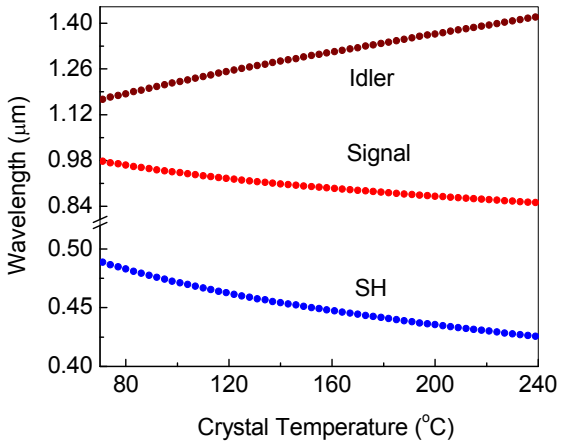

Fig. 2. Wavelength tuning range of the green-pumped MgO:sPPLT cw SRO and the corresponding frequency-doubled blue output as functions of crystal temperature for a grating period of 7.97 μm.

2.3 Blue power across the tuning range

We recorded the blue power near the maximum of the idler power for each crystal temperature by optimizing the input pump power before the onset of saturation [9]. Figure 3 (a) shows the extracted blue power across the tuning range. The measured power varies from 45 mW at 425 nm to 300 mW at 489 nm, with as much 448 mW available at 459 nm. We extracted >300 mW of blue power over 53% of the tuning range and >100 mW over 90% of the tuning range. The sudden fall in the blue power near 450 nm is due to the rise in signal coupling loss through mirror M_4, Fig. 3(b), which results in reduced intracavity signal power and thus lower SHG conversion efficiency, although there was no significant reduction in the idler power, Fig. 3(c). As the SRO is operating near saturation, a reduction in intracavity signal power does not have a significant impact on the idler power. As such, the use of a more optimized coating for M_4 with minimum transmission loss across the signal tuning range will readily overcome the dip in SH power. The overall decline in blue power towards the shorter wavelengths is, however, attributed to the reduction in intracavity signal power due to the increased effects of thermal lensing near the extremes of the SRO tuning range (higher temperatures), higher MgO:sPPLT crystal coating losses, and parametric gain reduction away from degeneracy, as observed previously [9]. The reduction of the intracavity signal power is also evident from the fall in idler power towards the extreme of the tuning curve, Fig 3(c).

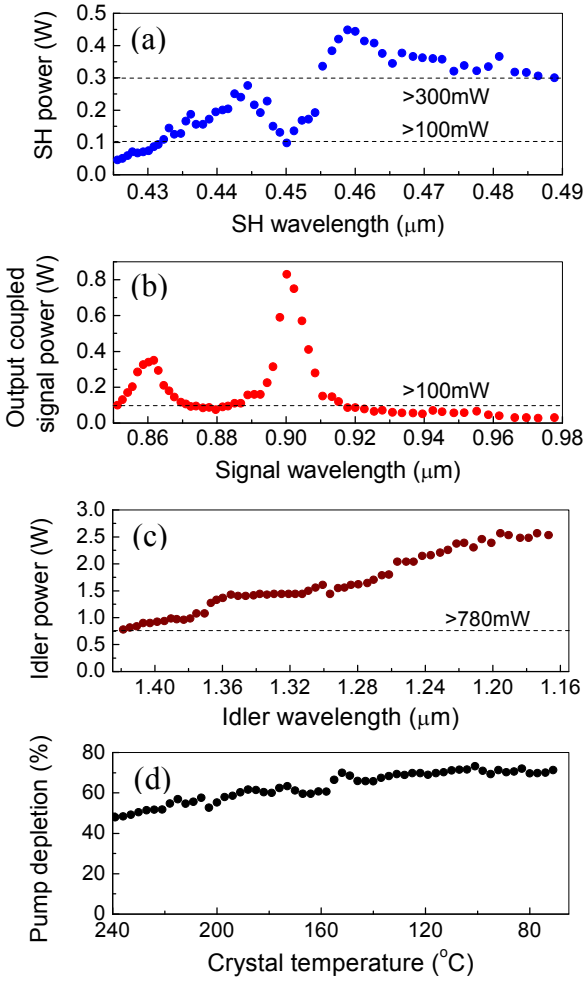

Fig. 3. (a) Second-harmonic blue power verses wavelength, (b) out-coupled signal power, (c) single-pass idler power and (d) corresponding pump depletion across the tuning range.

From the transmission data of the mirror M_4, and the out-coupled signal power, Fig. 3(b), we calculate that intracavity signal power to vary from ~170 W at 978 nm to ~35 W at 850 nm, representing a maximum single-pass SHG efficiency of 0.29%. As evident in Fig. 3(b), there is also >100 mW of useful signal output available over 850-915 nm (50% of total signal tuning range), with 830 mW at 900 nm. In addition to the blue and signal, the SRO simultaneously generates substantial levels of non-resonant idler powers of more than 780 mW, with as much as 2.6 W across the 1167 -1422 nm tuning range, as shown in Fig 3(c). Figure 3(d) shows the pump depletion across the tuning range. The measured pump depletion remains constant around 70% over 50% of the tuning range and drops to ~48% towards the extreme of the tuning range, a similar behavior to that observed our earlier reports [9].

2.4 Power scaling

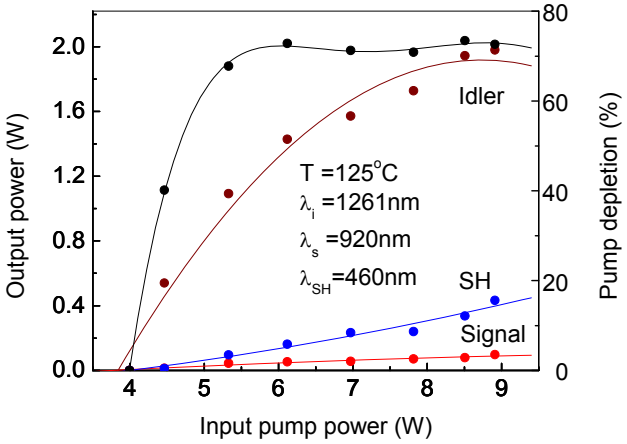

Fig. 4. Single-frequency blue power, signal power, idler power, and pump depletion as functions of input pump power to the frequency-doubled cw SRO. Solid lines are guides for the eye.

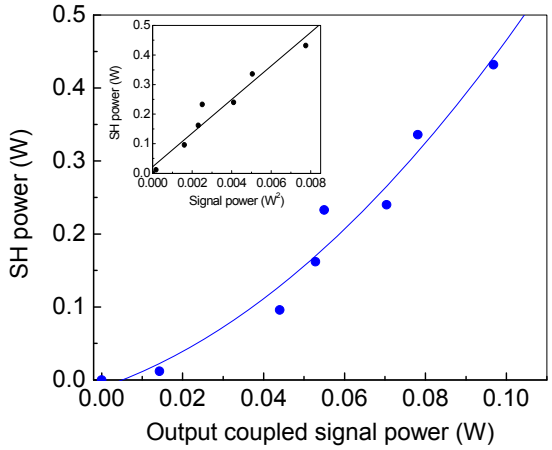

Fig. 5. Variation of SHG power with out-coupled signal power, showing a quadratic dependence. Inset: linear dependence of SHG power on the square of the out-coupled signal power.

We investigated the threshold and power scalability of the SRO near the maximum SHG power (at 460 nm), with the results shown in Fig. 4. At the maximum input pump power of 8.9 W, we obtained 432 mW of blue, 97 mW of out-

coupled signal, and ~1.98 W of idler power, with a corresponding pump depletion of ~73%. The SHG power exhibits a nearly linear rise with the input pump power. The pump power threshold for the frequency-doubled SRO is 4 W (2.4 W without the BIBO crystal). The rise in threshold is due to the reflection loss of the BIBO crystal faces at the signal. To gain further insight into the SHG process, we recorded the blue power as the function of the out-coupled signal power by varying the input pump power, with the results shown in Fig. 5. As expected, the increase in SHG power with out-coupled signal power is seen to be quadratic, also implying quadratic variation with the intracavity signal power. The inset of the Fig. 5 also confirms the linear variation in SHG power with the square of the out-coupled signal power, as expected. Using the linear slope efficiency one can in principle calculate the effective nonlinear coefficient (d_{eff}) of BIBO crystal, but the accuracy depends upon the estimation of the signal power inside the SRO which in tern upon the exact value of coupling coefficient of mirror, M_4.

3. 1.27-W, STABLE, CW, SINGLE-FREQUENCY BLUE GENERATION

The maximum available blue output power extracted from the frequency-doubled CW SRO described in section 2 is limited by the intracavity signal power and its spatial mode quality. As we are operating in the saturation region of SRO operation, we can not achieve further increases in signal power with increased pumping level. We can, however, attempt to improve the spatial mode quality of the resonating signal, as it is solely affected by thermal effects in the MgO:sPPLT nonlinear crystal due to the relatively large pump focusing parameter (ξ_{SRO}=2) [8,9]. Therefore, thermal effects, and thus the spatial beam quality of the signal, can be improved by using looser pump focusing along with a longer SRO cavity, in order to enhance the maximum blue output power.

3.1 Experimental configuration

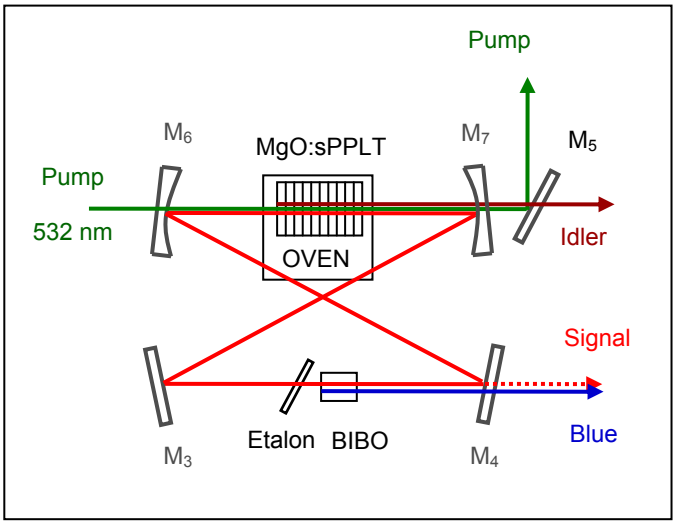

Fig. 6. Schematic of the intracavity frequency-doubled MgO:sPPLT cw SRO for watt-level blue generation.

Figure 6 shows the schematic of the experimental setup, which is similar to experimental configuration in Fig. 1. The ring cavity comprises two concave reflectors, M_6 and M_7, and two plane mirrors, M_3 and M_4. Unlike previous configuration, however, the mirrors M_6 and M_7 are of radius of curvature r=100 mm. All the mirrors have the same coating specifications as described in section 2, that is high reflecting (R>99.9%) for the resonant signal (840-1000 nm) and highly transmitting (T=85-90%) for the idler (1100-1400 nm), thus ensuring SRO operation. M_4 also has high

transmission (T=85-90%) over 425-500 nm. The nonlinear crystal is the same MgO:sPPLT (d_{eff}~10 pm/V) of length 30-mm with a single grating (Λ=7.97 μm). The pump is a frequency-doubled, cw, single-frequency Nd:YVO_4 laser. For internal SHG, we use BIBO as the nonlinear crystal and a 500-μm-thick uncoated fused silica etalon (FSR =206 GHz, finesse ~0.6) is used at the second cavity waist between M_3 and M_4 and adjacent to the BIBO crystal for frequency selection and mode-hop-free operation of the SRO. The BIBO crystal is 5 mm in length and cut for type I interaction ($ee \rightarrow o$) in the yz-plane (φ=90°) at an internal angle θ=160° at normal incidence (d_{eff}~3.4 pm/V). The crystal faces are AR-coated for the resonant signal (R<0.5%) and for the SHG wavelengths (R<0.8%). A lens of focal length 150 mm was used to focus the beam at the center of the crystal to a pump beam waist of ~33 μm (ξ=1.28) corresponding to a signal beam waist of ~39.55 μm at 900 nm. Calculated beam waist of the signal at the center of the BIBO crystal is 200 μm. The total optical length of the cavity including the crystals and etalon is 690 mm, corresponding to a FSR~434 MHz.

3.2 Power across the tuning range

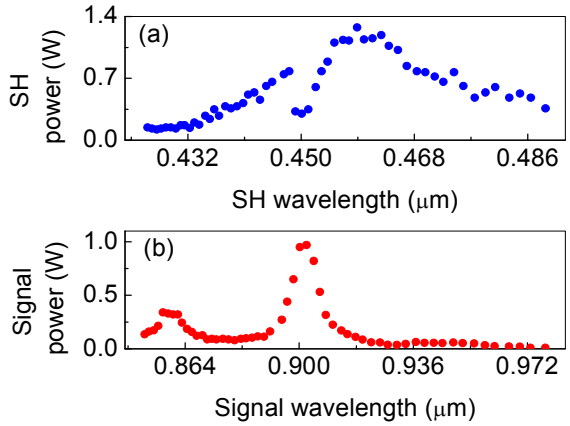

Fig. 7. (a) Generated blue power versus wavelength, and (b) Out-coupled signal power across the tuning range.

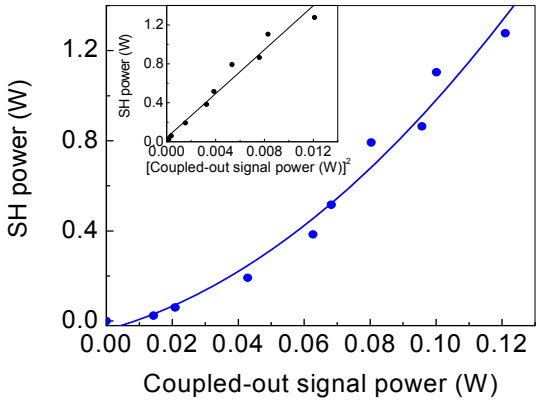

Fig. 8. Quadratic dependence of SHG power on out-coupled signal power. Inset: linear dependence of SHG power on the square of the out-coupled signal power.

By varying the MgO:sPPLT crystal temperature from 71 °C to 240 °C, the signal could be tuned from 978 to 850 nm. The corresponding SHG wavelengths from 489 to 425 nm are generated by varying the BIBO crystal angle from 163.8° to 155.2°. Figure 7 (a) shows the extracted SH blue power across the tuning range. The measured power varies from 145

mW at 425 nm to 360 mW at 489 nm, with as much 1.27 W available at 459 nm with a green to blue conversion efficiency in excess of 14% at crystal temperature 128°C. We extracted >500 mW of blue power over 58% of the tuning range and >250 mW over 84% of the tuning range. The sudden fall in the blue power near 450 nm is due to the rise in signal coupling loss through mirror M_4, which results in reduced intracavity signal power and thus lower SHG conversion efficiency. As such, the use of a more optimized coating for M_4 with minimum transmission loss across the signal tuning range will readily overcome the dip in SHG power. The overall decline in blue power towards the shorter wavelengths is, however, attributed to the reduction in intracavity signal power due to the increased effects of thermal lensing near the extremes of the SRO tuning range (higher temperatures), higher MgO:sPPLT crystal coating losses, and parametric gain reduction away from degeneracy, as observed previously. As evident in Fig. 7(b), there is also >100 mW of useful signal output available over 850-915 nm (50% of total signal tuning range), with 970 mW at 900 nm. In addition to the blue and signal radiations, the SRO simultaneously generates substantial levels of non-resonant idler radiation with powers of more than 780 mW, with as much as 2.6 W across the 1167-1422 nm tuning range.

Figure 8 shows the blue power at 459 nm as the function of the out-coupled signal power by varying the input pump power. As expected, the increase in SHG power with out-coupled signal power is seen to be quadratic, also implying quadratic variation with the intracavity signal power. The inset of the Fig. 8 also confirms the linear variation in SHG power with the square of the out-coupled signal power, as expected.

3.3 Stable single-frequency operation

We analyzed the spectrum of the generated blue light using a confocal scanning Fabry-Perot interferometer (FSR=1 GHz, finesse=400). A typical transmission fringe pattern at maximum blue power at 459 nm is shown in Fig. 9, confirming single-frequency operation with an instantaneous linewidth of ~8.5 MHz. Similar behaviour was observed throughout the tuning range in the blue. In the absence of active frequency control, we recorded mode-hope-free, single-mode behavior of the blue output using a wavemeter (BRISTOL 612A, resolution 0.2 pm). As evident in Fig. 10, passive frequency-stability of the system is better than 280 MHz (limited by the wavemeter resolution) over a time-scale of 340 seconds, implying the possibility of stable single-frequency operation over longer time with active stabilization and improved thermal isolation of the system from the laboratory environment.

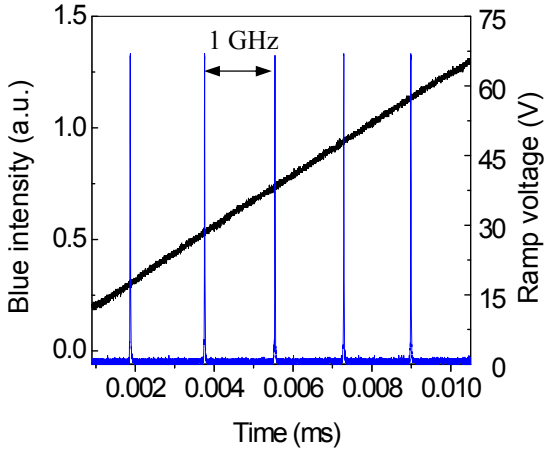

Fig. 9. Single-frequency spectrum of the generated blue light recorded by a scanning Fabry-Perot interferometer.

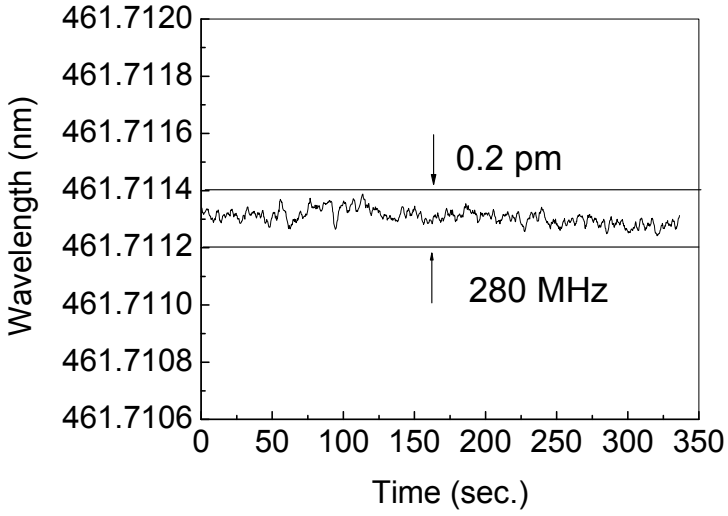

Fig. 10. Wavelength stability of the single frequency blue radiation over time. The crystal temperature was fixed at 128°C corresponding to a signal wavelength of 923 nm.

3.4 Beam profile

The far-field energy distribution of the blue beam at 460 nm, together with the intensity profile and the Gaussian fits along the two orthogonal axes, are shown in Fig. 11. The oblique line pattern on the color beam plot is interference fringes caused by attenuation optics used to reduce blue intensity to the beam profiler. The beam intensity profile along the two orthogonal axes appears to confirm a Gaussian distribution, although full confirmation of TEM_{00} character requires measurements of M^2 values. The ellipticity of the spot is 0.69, attributed to spatial walk-off as well as the astigmatism of the signal beam caused by the relatively large tilt angles (15°) on M_1 and M_2 to extract the blue beam out of the compact ring cavity.

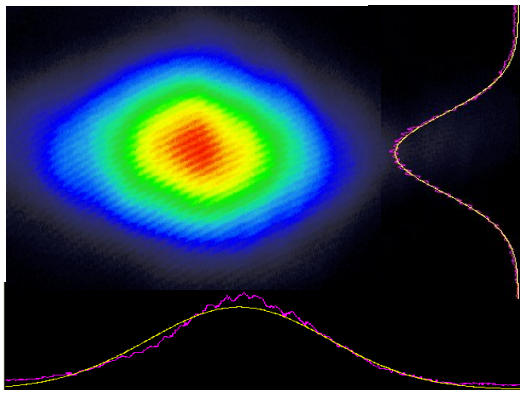

Fig. 11. TEM_{00} energy distribution, beam profiles, and Gaussian fits of the generated green beam in the far-field.

4. GENERATION OF TUNABLE FEMTOSECOND PULSES IN THE ULTRAVIOLET

4.1 Experimental configuration

The configuration of the intracavity frequency-doubled BIBO femtosecond OPO is shown in Fig. 12. The OPO is synchronously-pumped by the second-harmonic of a KLM Ti:sapphire laser at 415 nm. The laser provides 2.1 W of average power at 830 nm in ~150 fs pulses at 76 MHz. Single-pass SHG in a 1-mm-long BIBO crystal cut at θ=152° for type I (*ee*→*o*) phase-matching in the optical *yz* plane provides 1.15 W of average power in the blue at ~55% efficiency [5,6]. The blue pump pulses at 415 nm, determined by autocorrelation measurements in a 200-μm β-BaB_2O_4 (BBO) crystal cut for type I (*oo*→ *e*) phase-matching at θ=80°, have durations of ~180 fs. The OPO resonator is modified from our earlier work [10] by the inclusion of an additional focusing section for the doubling crystal. The cavity is now a bifocal ring, comprising four concave reflectors (*r*=100 mm) and two plane mirrors. The concave mirrors M_1 and M_2 provide the focus for the OPO crystal, whereas M_5 and M_6 allow focusing into the SHG crystal. All mirrors are >99% reflecting for visible signal wavelengths over 500-700 nm. M_1 and M_2 are also >90% transmitting for the blue pump over 380-450 nm. The ring resonator allows the generation of the UV output in one direction through M_6. To allow maximum UV extraction, M_6 also has high, but variable transmission (*T*~70% to 90%) over 250-350 nm.

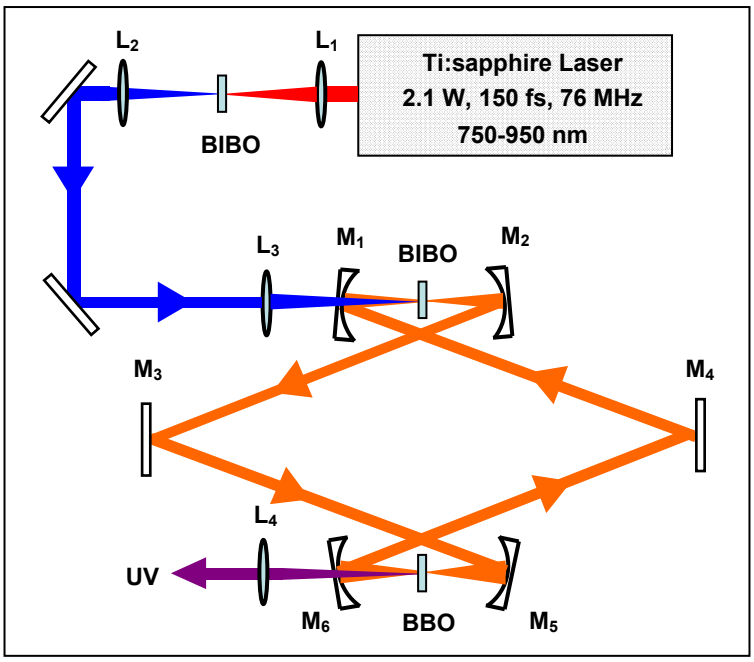

Fig. 12. Configuration of the intracavity frequency-doubled visible BIBO femtosecond OPO synchronously pumped by the second harmonic of KLM Ti:sapphire laser in the blue. L_1 and L_3: focusing lenses; L_2 and L_4: collimating lenses.

4.2 Tuning of intracavity frequency-doubled femtosecond OPO in the UV

Wavelength tuning in the UV was achieved by continuous tuning of the OPO signal across the visible through angular rotation of the BIBO crystal and simultaneous angular tuning of the BBO second harmonic crystal. At each wavelength, the cavity was optimized to compensate for any lateral shifts due to angular tuning or changes in synchronous length in order to achieve maximum UV output. The OPO signal could be tuned across 500-710 nm by changing the internal BIBO crystal angle from θ=171.5° to θ=154.5°, with the corresponding UV wavelength range of 250 to 355 nm generated for a change in the internal angle of the BBO crystal from θ=52.3° to θ=33.1°. The limit to the obtained tuning

range in the UV was set by the overall reflectivity of the cavity mirrors at the signal wavelength. By using mirrors with broader reflectivity band and shorter pump wavelengths near 400 nm, coverage across 230-360 nm should be attainable.

4.3 Spectral characteristics of UV radiation

Figure 13 shows recorded spectra of the visible signal and the second harmonic in the UV. As can be seen from Fig. 13(a), the visible signal spectral widths typically vary between ~3 nm to ~3.5 nm. At shorter signal wavelengths in the green, however, the bandwidth is broadened to ~8 nm, which we attribute to the net OPO cavity dispersion in this range in the absence of intracavity dispersion control. Combined with self-phase-modulation, this leads to spectral broadening and chirping of the signal pulses in the green. Nevertheless, the UV spectra exhibit consistent behavior, with bandwidths from ~0.5 nm to ~1 nm across the tuning range. The bandwidth reduction from the visible to the UV is attributed to the spectral acceptance for phase-matching in BBO, which results in gain narrowing, thus constraining the second harmonic conversion bandwidth for the fundamental pulses. The calculated spectral acceptance bandwidth for SHG in the 500-μm BBO crystal varies from ~1 nm to ~5 nm over the fundamental range of 500 nm to 700 nm, implying stronger spectral narrowing at shorter signal wavelengths. Accordingly, stronger reduction in the UV spectral bandwidths towards the shorter wavelengths is expected. This is qualitatively supported by the recorded spectra in Fig. 13(b). Further spectral narrowing from the visible to the UV is also to be expected from the nonlinear nature of gain in the SHG process.

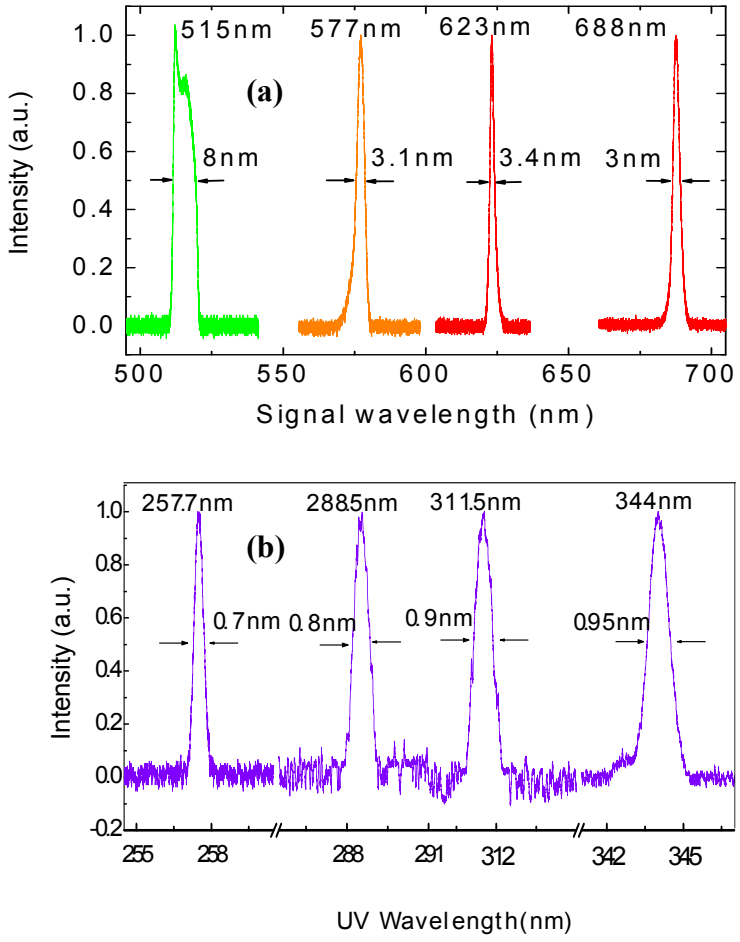

Fig. 13. Typical spectra of (a) the visible signal, and (b) the corresponding generated second harmonic in the UV.

4.4 Power scaling of UV output

We were able to generate UV average powers in excess of 175 mW over ~70% of the tuning range (275-350 nm) and more than 100 mW over ~80% of the tuning range (270-355 nm). In the wavelength range of 255-270 nm, practical powers of 25 to 100 mW were still generated, with 5 mW available at 250 nm. We believe the decline in the generated UV power below 270 nm is mainly due to the spectral broadening and chirping of visible signal pulses in the green as described above. Together with the decrease in spectral acceptance for phase-matching in BBO towards shorter wavelengths, this results in reduced UV power in these regions. The highest UV average power was obtained at 323 nm. Figure 14 shows a plot of the generated UV power and conversion efficiency at 323 nm versus pump power at 415 nm. The generated UV power can be seen to increase almost linearly, reaching 225 mW at the maximum available blue power of 1.15 W, representing a conversion efficiency of 19.7%. The UV power of 225 mW is close to the maximum visible signal power of 270 mW extracted directly from the OPO previously [10], implying that the intracavity doubling acts as an almost optimized nonlinear coupler for the signal. Given the linear rise in power and no evidence of saturation, we can expect higher UV output powers in excess of 225 mW with higher input pump powers. The short lengths of BIBO and BBO crystals resulted in minimum beam distortion arising from the effects of spatial walkoff, tight focusing or cavity astigmatism, so that the UV output beam had close to a circular profile with a M^2<1.1. The blue pump power threshold for the frequency-doubled OPO was as low as 150 mW, equivalent to a fundamental Ti:sapphire laser power of 600 mW.

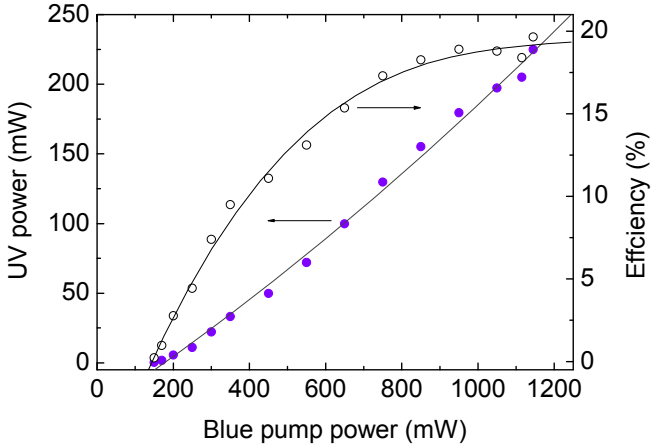

Fig. 14. Variation of the generated UV average power and conversion efficiency at 323 nm with the blue pump power at 415 nm.

4.5 Temporal characteristics of UV pulses

Temporal characterization of the generated UV pulses was performed using the cross-correlation technique. The UV pulses were mixed with 150-fs Ti:sapphire fundamental pulses at 830 nm in a 500-μm-thick BBO crystal cut at θ =26° for type I ($o+o\rightarrow e$) phase-matching. Background-free cross-correlation intensity profiles were obtained using a GaAsP detector. A typical cross-correlation profile and the corresponding spectrum at 323 nm are shown Figure 15, confirming a near-transform-limited pulse with a time-bandwidth product $\Delta\nu.\Delta\tau$ ~0.34, assuming sech^2 pulse shape. Across the UV tuning range, pulse durations of 132 fs to 250 fs were measured, with corresponding time-bandwidth products varying from $\Delta\nu.\Delta\tau$ ~0.34 to $\Delta\nu.\Delta\tau$ ~0.6.

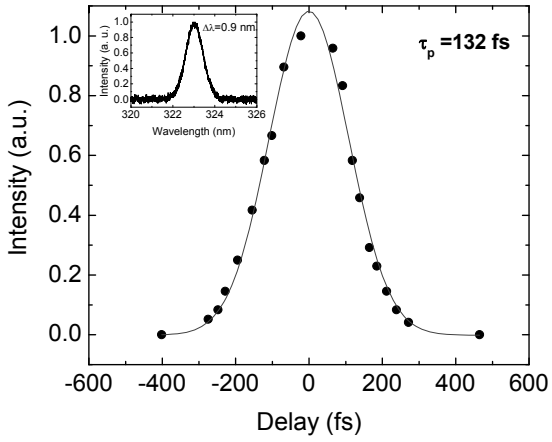

Fig. 15. Cross-correlation trace, and (inset) spectrum of the generated UV pulses at 323 nm. The time duration of $\Delta\tau$ ~132 fs and the spectral bandwidth of $\Delta\nu$~0.9 nm result in near-transform-limit pulses with a time–bandwidth product of $\Delta\nu.\Delta\tau$~0.34.

5. CONCLUSIONS

We have demonstrated practical solid-state sources blue and UV radiation in the cw and ultrafast femtosecond regime using intracavity frequency doubling in cw and synchronously-pumped SROs. In cw operation, we have demonstrated tuning across the 425-489 nm spectral range in the blue and in femtosecond regime, we have achieved tuning over 250-355 nm in the UV. Intracavity frequency doubling of the cw SRO based on MgO:sPPLT has enabled the generation of up to 1.27 W of single-frequency blue output along with >100 mW of useful signal over 850-915 nm, with 970 mW at 900 nm, and non-resonant idler powers of more than 780 mW, with as much as 2.6 W across the 1167-1422 nm. The demonstrated tuning range of the blue is limited by the grating period of the MgO:sPPLT crystal, and so can be extended to cover the entire range of 300-530 nm using alternative gratings. The use of other grating periods will also enable blue generation at lower temperatures, reducing the effects of thermal lensing, and thus extending the higher powers to shorter wavelengths. Moreover, by resonating the idler wave in the 1140-1420 nm range, tunable generation across the 570-710 nm will also be possible, making this a promising approach for the generation of high-power, widely tunable, cw radiation across the 300-700 nm spectral range. Intracavity frequency-doubling of a visible femtosecond OPO based collinear phase-matching in BIBO has permitted the generation of high-repetition-rate femtosecond pulses across 250–355 nm in the UV at 225 mW of average power using angle tuning at room temperature, a single set of optics, and only two tuning parameters. The demonstrated wavelength coverage of UV can be further extended down to 230 nm by improving the mirror coatings and by using shorter pump wavelength near 400 nm. With the inclusion of intracavity dispersion compensation, we also expect further enhancements in the UV power at shorter wavelengths and transform-limited pulses throughout the tuning range. The significant spectral coverage in the blue and UV, practical powers, high spatial, spectral and temporal output beam quality, and potential for further wavelength extension throughout the visible and UV make the described sources highly attractive for a wide range of applications in a variety of scientific and technological applications in spectroscopy, optical communications, biophotonics, and nanotechnology.

ACKNOWLEDGEMENTS

This work was supported by the Ministry of Education and Science of Spain through grant TEC2006-12360 and through the Consolider program (CSD2007-00013).

REFERENCES

[1] Sakai, K., Koyata, Y., and Hirano, Y., "Blue light generation in a ridge waveguide MgO:$LiNbO_3$ crystal pumped by a fiber Bragg grating stabilized laser diode," Opt. Lett. 32, 2342-2344 (2007).

[2] Czeranowsky, C., Heumann, E., and Huber, G., "All-solid-state continuous-wave frequency-doubled Nd:YAG–BIBO laser with 2.8-W output power at 473 nm," Opt. Lett. 28, 432-434 (2003).

[3] Xue, Q. H., Zheng, Q, Bu, Y. K., Jia, F. Q., and Qian, L. S., "High-power efficient diode-pumped Nd:YVO_4 /LiB_3O_5 457 nm blue laser with 4.6 W of output power," Opt. Lett. 31, 1070-1072 (2006).

[4] Falcoz, F., Balembois, F., Georges, P., Brun, A., and Rytz, D., "All-solid-state continuous-wave tunable blue-light source by intracavity doubling of a diode-pumped Cr:LiSAF laser," Opt. Lett. 20, 1274-121276 (1995).

[5] Ghotbi, M., and Ebrahim-Zadeh, M., "Optical second harmonic generation properties of BiB_3O_6," Opt. Express 12, 6002-6019 (2004).

[6] Ghotbi, M., Ebrahim-Zadeh, M., Majchrowski, A., Michalski, E., Kityk, I. V., "High-average-power femtosecond pulse generation in the blue using BiB_3O_6," Opt. Lett. 29, 2530-2532 (2004).

[7] Rotermund, F., and V. Petrov, V., "Generation of the fourth harmonic of a femtosecond Ti:sapphire laser, " Opt. Lett. 23, 1040-1042 (1998).

[8] Samanta, G.K., Fayaz, G. R., Sun, Z., and Ebrahim-Zadeh, M., "High-power, continuous-wave, singly resonant optical parametric oscillator based on MgO:sPPLT," Opt. Lett. 32, 400-402 (2007).

[9] Samanta, G.K., Fayaz, G. R., and Ebrahim-Zadeh, M., "1.59W, single-frequency, continuous-wave optical parametric oscillator based on MgO:sPPLT," Opt. Lett. 32, 2623-2625 (2007).

[10] Ghotbi, M., A. Esteban-Martin, A., and Ebrahim-Zadeh, M., "BiB_3O_6 femtosecond optical parametric oscillator," Opt. Lett. 31, 3128-3130 (2006).

[11] Yanovsky, V. P., and Wise, F. W., "Frequency doubling of 100-fs pulses with 50% efficiency by use of a resonant enhancement cavity," Opt. Lett. 19, 1952-1954 (1994).

[12] Gale, G. M., Cavallari, M., Driscoll, T. J., and Hache, F., "Sub-20-fs tunable pulses in the visible from an 82-MHz optical parametric oscillator," Opt. Lett. 20, 1562-1564 (1995).

[13] Ghotbi, M., and Ebrahim-Zadeh, M., "990 mW average power, "52% efficient, high repetition- rate picosecond-pulse generation in the blue with $BiB3O_6$," Opt. Lett. 30, 3395-3397 (2005).